



university of
 groningen

faculty of science
 and engineering

kapteyn astronomical
 institute

UNIVERSITY OF GRONINGEN

BACHELOR THESIS DISSERTATION

Tactile Models from Astronomical Imaging Data

Author:
Thijs van Beers

Supervisor:
Dr. Jake Noel-Storr
Second examiner:
Dr. Kateryna Frantseva

2 July 2021

Abstract

This thesis aims to make astronomy more accessible, in particular to tactile learners as well as visually impaired and blind people, by providing methods to generate tactile models from astronomical imaging data that can be 3D printed. A complete procedure will be given starting from observational imaging data and ending at 3D printed tactile model. The steps include image processing for both image quality and model quality, choosing model settings and 3D printer settings. An interface has been developed which can be used to process images and generate models easily. To ensure the accessibility of the interface for visually impaired and blind people, it is compatible with screenreaders.

Acknowledgements

First I would like to thank Dr. Jake Noel-Storr for being a very involved supervisor and bringing together a great group, even in pandemic times. I would also like to thank all the Observational Astronomy students who have let me use their data, it was instrumental to my project. A big thank you also to my group of 3D printer friends from DJO, with whom I have built my printer and learned a lot of the required knowledge to do this project. And of course thanks to my parents who drove me there so many times. I want to thank Wouter and Lasse for making going to university so fun. And finally, thank you Emma for your support in both my academic and personal life.

Contents

1	Introduction	3
1.1	Accessibility in Science and Education	3
1.2	Tactile Learners	4
1.3	Goal	4
2	Astronomical Imaging	5
2.1	Observational Data	5
2.2	Image Processing	5
3	3D Printing	13
3.1	FFF printing	13
3.2	Slicing	14
4	Tactile Models	15
4.1	Modelling from Imaging Data	15
4.2	3D Printing Limitations and Solutions	17
4.2.1	Downscaling the image	17
4.2.2	Printer and model settings	17
4.2.3	Image Processing	21
4.2.4	Draft model	23
5	Interface	26
5.1	Main window	26
5.2	Panels	27
6	Conclusion & Discussion	29
	Bibliography	31

Chapter 1

Introduction

Historically, astronomy is an inherently visual science. To satisfy curiosity about something in the sky, taking a look what can be seen at night or pointing a telescope at it are very logical steps to take. This observational character has propagated through to today, where still many fields of astronomy rely on observational imaging to do their science and in the public astronomy eye is often represented with grand images of galaxies and nebulae. This way of visual communication is for many an entry point in astronomy or a reason to love the subject, but unfortunately, for some, it can also be a big obstacle to overcome and a reason that is keeping them away from astronomy.

1.1 Accessibility in Science and Education

For blind and visually impaired (VI or BVI) people, image based science and education is a constraint. In education, a big challenge is the lack of adapted materials to replace or enhance the already available visual materials. [Yuen et al., 2004] A study by Rule et al. [2011a] found that teachers that aren't introduced yet to such materials are not confident they can provide students with visual impairment the same quality of education as non-impaired students. Research into tactile solutions for this lack of material have been promising. Sahin and Yorek [2009] named tactile models alongside audio recordings and Braille note-taking devices as needed materials for teaching science to VI students. Also Rule [2011b] and Hasper et al. [2015] have found success when using tactile models to teach STEM subjects, including astronomy.

In STEM employment BVI are severely under represented. Of BVI clients that found employment through vocational rehabilitation programs in the United States, only 5% ended up in STEM field with even less in scientific fields. [Cavanaugh et al., 2006] [Blackorby et al., 2003]

1.2 Tactile Learners

While the necessity for tactile materials in science and education is to support BVI, research into these tools shows they can also be applied more broadly. Rule [2011b] found that sighted students that interacted with these materials also improved their understanding of the subject, tying the results to different learning styles. The concept of learning styles is that different people and subjects require different teaching methods and that these can be classified as learning styles. [Pashler et al., 2008] More successes of tactile materials originally designed for BVI students were found by Hasper et al. [2015] and by teachers given such materials. [Rule et al., 2011a]

1.3 Goal

Most of the research mentioned above has been conducted in primary and secondary education. There have also been outreach projects such as *Tactile Universe* by Bonne et al. [2018], that aim to make astronomy accessible to the broader BVI public. The aim of this project will be to supplement those efforts with more academic material and tools.

In this thesis methods and procedures will be researched that focus not just on accessibility of education in astronomy, but on making the practice of astronomy more accessible. More specifically the practice of observational astronomy, by providing tactile models generated from observational astronomical imaging. The tactile models will be 3D printed, but there will be a focus on keeping the procedures as accessible as possible. This means a novice ¹ to 3D printing should be able to apply the procedures discussed. This project will work towards providing a complete path from telescope observation to tactile model, focussing on image processing steps as well as techniques for creating and printing the tactile models. As the models can be useful for sighted tactile learners as well as BVI and there are many types of visual impairment, no level of sightedness is assumed.

¹Someone that has successfully sliced and printed at least one object and has access to a 3D printer.

Chapter 2

Astronomical Imaging

2.1 Observational Data

For this project test data to develop into models had to be sourced. For some early tests of the basic image to model algorithm an image of the Sombrero galaxy (NGC 4594) from the Sloan Digital Sky Survey was used, in particular from data release 8 which included data from SDSS-III. [Eisenstein et al., 2011] [Aihara et al., 2011] This image was useful for early test as it was already processed and the object was very visible.

To develop a more complete process from telescope to model, images were sourced from astronomy students at the University of Groningen who kindly lend their data for this project. The images sourced from them were specifically chosen to only be adjusted for basic observational effects, but not yet processed in any other way. The images were taken using the Blaauw Observatory's Gratama Telescope, a 40 cm Cassegrain telescope of the Ritchey-Chrétien type.

Each image has been adjusted for dark current, an effect where thermal excitation increases the value of a pixel instead of photon excitation. A frame of no exposure, called a bias frame, which adjust for the bias level of each pixel has also been subtracted from the image. To adjust for the differences in gain between the pixels a flatfield image of a uniform blank screen on the inside of the dome around the telescope was taken and the image is divided by it. A measure of how much atmosphere is above the telescope at the time of observing, called the airmass, is also corrected for. Lastly multiple exposures of the same object in the same colour band are combined to create one image.

2.2 Image Processing

After the image is adjusted for observational effects, although it is a numerically accurate image of the observed object, it is often not yet visually useful.

Typically the entire image is still very dark and the object is too faint to see, also if linearly scaled. Other problems can be noise in the background sky, cosmic rays and, in the case of observing galaxies, bright foreground stars. In order to address these issues there are many tools and algorithms available, for this project a selection of algorithms from the `scikit-image` Python package is used. [van der Walt et al., 2014] Some of these algorithms can also be used to prepare an image that can be more easily or better 3D printed as a tactile model, but this will be discussed in a later chapter. Here, an overview of the methods used in this project will be given in the context of astronomical image processing. In figures 2.1 through 2.6 applied examples of the algorithms can be found.

Chop

A chop refers to setting a floor or ceiling value for the brightness in an image. All values below the floor or above the ceiling are capped to the floor or ceiling respectively. This algorithm is not part of the `scikit-image` python package, but can be performed in Python mathematically. It can be useful to eliminate noise in the background sky, by setting a floor value such that it is above most of the noise but below the values of the observed object. A ceiling value can be useful to set when particularly bright objects push other objects into the background, for instance, when observing a cluster in which a few stars overshadow the others.

Equalize histogram

The equalize histogram algorithm implemented by `scikit-image` flattens the histogram of an image so that all values are as equally common as possible. [Solem, 2009] The algorithm uses the cumulative distribution function (cdf), which is calculated by summing over the histogram from dark to bright. Then the brightness values of each pixel is mapped to the corresponding normalized cdf value, which can be written as a new assigned value O for each brightness value I in the original image.

$$O = \sum_{i=0}^I n_i / N \quad (2.1)$$

Where n_i is the number of pixels of brightness value i in the original image and N is the total number of pixels. This means it increases contrast as it spreads out areas of the histogram where a lot of values are close together and the cdf increases rapidly. An unintended effect can be that noise with a small variation is also spread out.

Gamma correction

The gamma correction algorithm follows the following simple equation:

$$O = I^\gamma \quad (2.2)$$

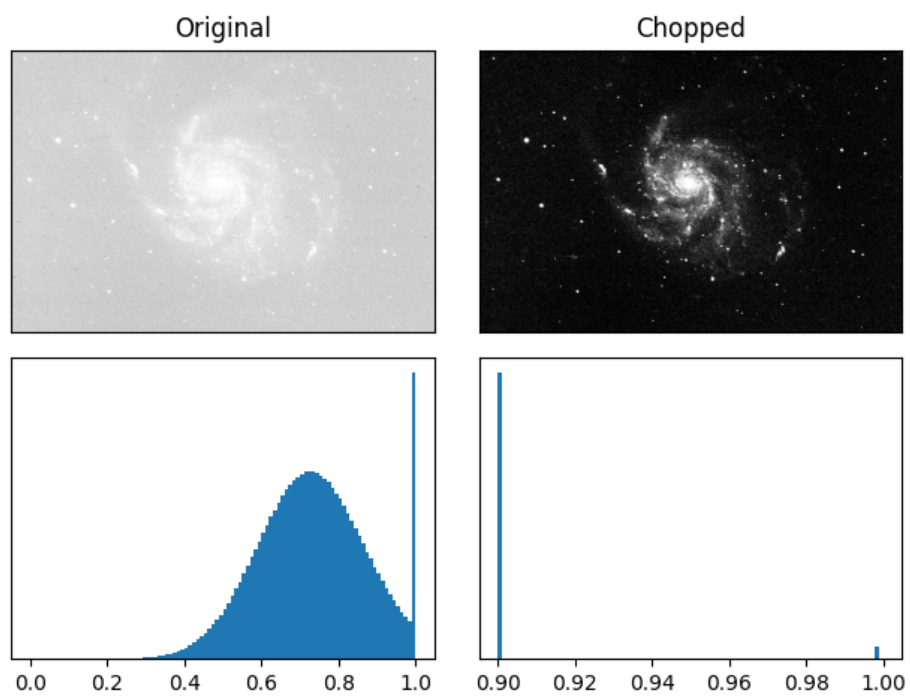


Figure 2.1: The chop algorithm applied to an image of M101, with a floor of 0.9 set. Underneath the images their histograms are shown.

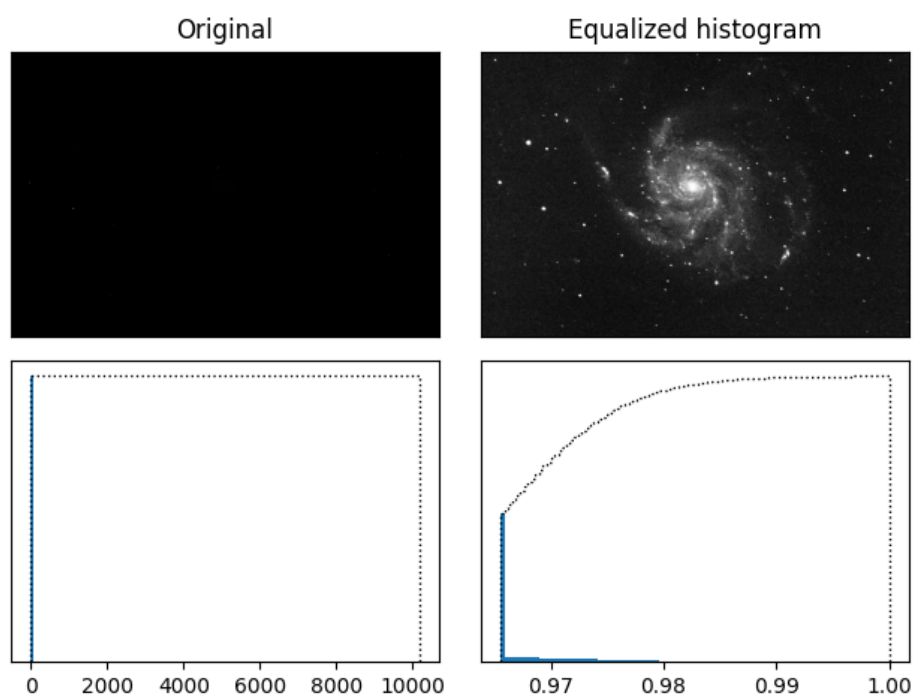


Figure 2.2: The equalize histogram algorithm applied to an image of M101. Underneath the images their histograms are shown, with the cumulative distribution function as a dotted line on top.

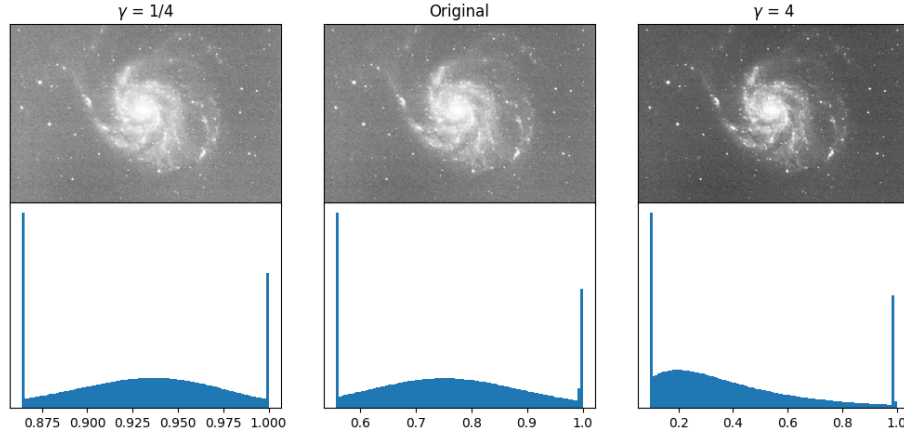


Figure 2.3: The gamma correction algorithm applied to an image of M101 for both a value of gamma above and below 1. Underneath the images their histograms are shown.

Where O is the output image, I is the input image scaled to have values from 0 to 1 and γ is an adjustable non negative parameter. The equation is applied to the image pixelwise. For values of γ smaller than 1, the image will appear brighter. For the astronomical use case a γ of value greater than 1 is more common, in order to make the background sufficiently dark.

Log correction

Another algorithm that follows a simple equation is the log correction, following

$$O = G \cdot \log_2(1 + I) \quad (2.3)$$

Where O and I are again the output and input scaled to have values from 0 to 1 respectively. G is the gain, an adjustable parameter. The equation is applied to the image pixelwise. This algorithm is useful to make the more faint parts of objects visible. It also creates a more intuitive representation of the object at increased brightness, as people experience brightness on a logarithmic scale which a regular linear amplification would not have adjusted for.

Total variation denoise

If the image still contains a lot of noise, a total variation denoise algorithm can be applied. This algorithm seeks to find a balance between approximating the original image and minimizing the total variation in the approximation. [Chambolle, 2004] The total variation $J(O)$ of image O of size $N \times N$ is given by

$$J(O) = \sum_{1 \leq i, j \leq N} |(\nabla O)_{i,j}| \quad (2.4)$$

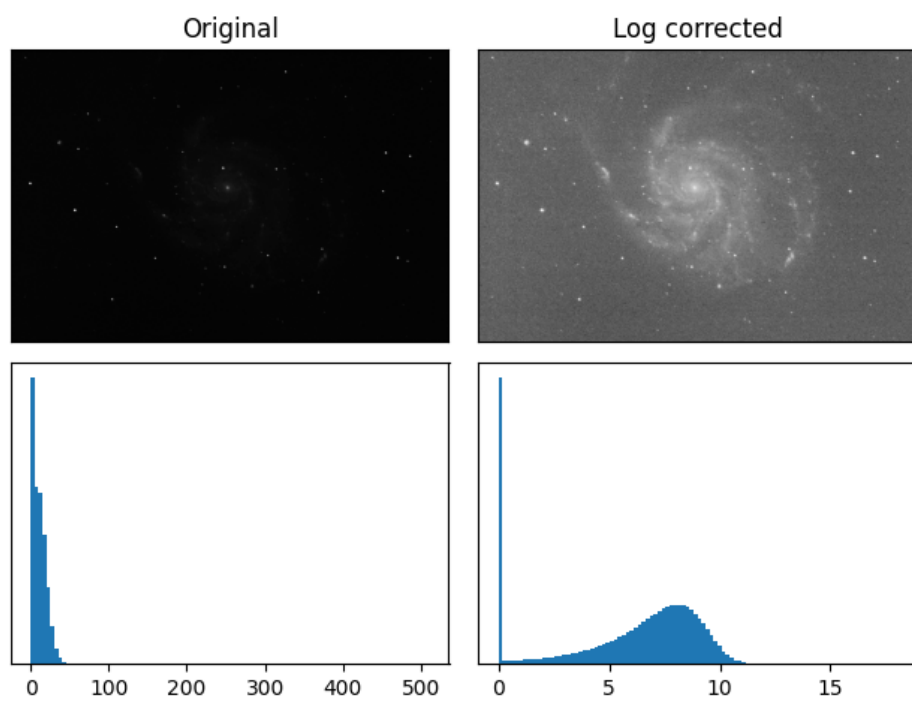


Figure 2.4: The log correction algorithm applied to an image of M101. Underneath the images their histograms are shown.

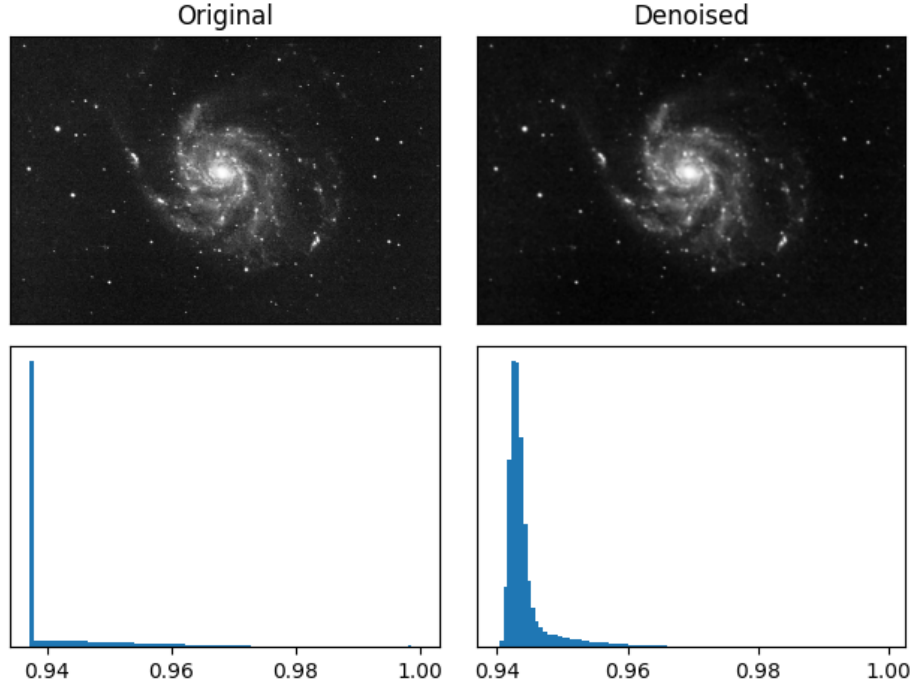


Figure 2.5: The total variation denoise algorithm applied to an image of M101. Underneath the images their histograms are shown.

Where

$$(\nabla O)_{i,j} = ((\nabla O)_{i,j}^1, (\nabla O)_{i,j}^2)$$

with

$$\begin{aligned} (\nabla O)_{i,j}^1 &= \begin{cases} O_{i+1,j} - O_{i,j} & \text{if } i < N, \\ 0 & \text{if } i = N, \end{cases} \\ (\nabla O)_{i,j}^2 &= \begin{cases} O_{i,j+1} - O_{i,j} & \text{if } j < N, \\ 0 & \text{if } j = N, \end{cases} \end{aligned}$$

The equation it tries to minimize is

$$\frac{\|O - I\|^2}{2\lambda} + J(O) \quad (2.5)$$

Where I is the input image, O is the output image, $\|\cdot\|$ is the Euclidean norm in $\mathbb{R}^{N \times N}$ and λ is a weight controlling how strong the denoising is. The exact algorithm implemented in the `scikit-image` package is that of Chambolle [2004]. The algorithm includes the weight as an adjustable parameter.

Remove foreground stars

Lastly there are cases in which it is desired to remove foreground stars from an image, for example in an image of a galaxy. This can be done by

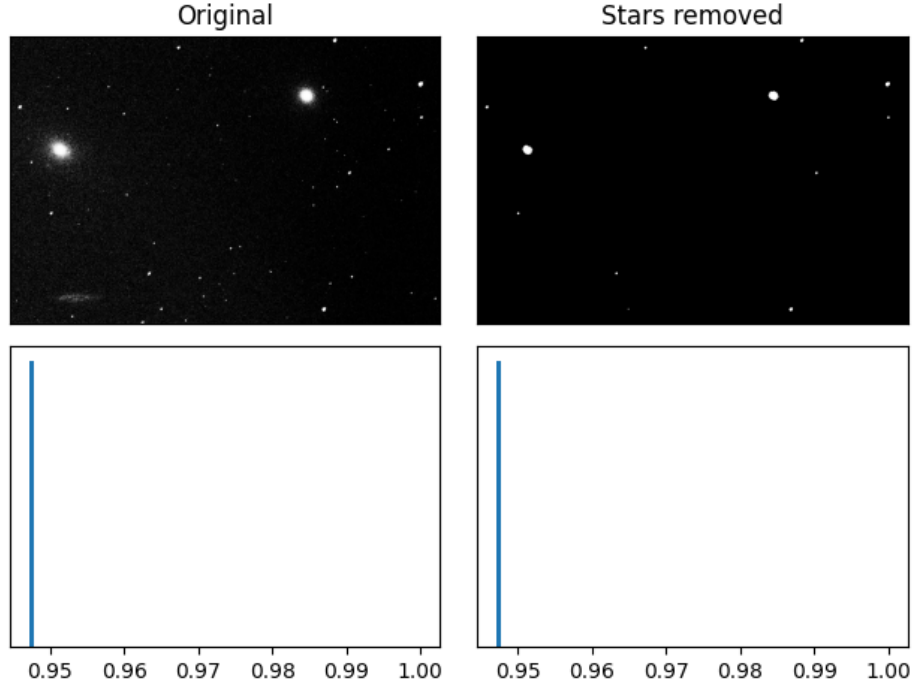


Figure 2.6: An image of part of the Virgo cluster from which foreground stars have been removed with a white top-hat transform. Underneath the images their histograms are shown.

using a white top-hat transform, this transform finds bright spots in the image that fit within the so called structuring element. [Tcheslavski, 2010] The equation for the top-hat transform of image I with structuring element s is

$$T_{\text{hat}}(I) = I - (I \circ s) \quad (2.6)$$

Where \circ is the morphological opening operator. The structuring element used in this case a disk of which the radius is an adjustable parameter, using this stars of an adjustable maximum size can be found by the white top-hat. The output image with the stars removed is then this white top-hat subtracted from the original image.

Chapter 3

3D Printing

This chapter will give a general introduction to the 3D printing process, focussing on FFF printing which is the most relevant for this project. It will also discuss some of the limitations of the technology as well as some common techniques that are used to ensure successful prints.

The specific 3D printers that have been used in this project are a RepRap Prusa Mendel i2 [Prusa, 2011] and LABIST X1 [LABIST]. The methods and models in the project will however be compatible with any FFF printer and no settings or procedures that are specific to these printers are discussed.

3.1 FFF printing

Fused filament fabrication (FFF), also known as fused deposition modeling (FDM), is a method of producing objects from thermoplastic polymers. [Jones et al., 2011] FFF 3D printers consist of an extruder, a bed and some assembly to move them along three axis, typically the extruder moves in two axis and the bed in the remaining one. As convention the horizontal plane of the bed is considered the XY-plane and the vertical direction the Z-axis. The extruder is fed a plastic filament, which it melts so it can extrude molten plastic onto the bed. By moving the extruder with respect to the bed in the XY-plane during this process a shape is drawn. The extruder then moves up slightly in the Z-axis so it can draw another layer on top of the previously drawn shape. Layer by layer this builds up the object it is printing.

Because of this layer by layer approach to creating an object, the printer always needs something to print on top of. Because of this, objects with parts that have no connection underneath them are difficult or even impossible to print. These unsupported parts are called *overhangs*. Typically short gaps can be bridged and angles up to about 45° are printable. Another consequence of layer by layer printing shows when in some cases the extruder will move between different areas of a layer to print different fea-

tures. As the extruder moves it tries not to extrude plastic, but often a small filament of molten plastic is still drawn from one feature to another. The resulting effect of a print with many plastic strings between features is called *stringing*.

In this project other types of printers such as stereolithography (SLA) printers that print in resin are not specifically considered as FFF printers are the most common and are cheaply available. The 3D model files created for this project could however be prepared for and printed on any type of printer.

3.2 Slicing

To 3D print an object, it is needed as a digital model, such as an STL file which describes the surface of the object as a triangle mesh. The process of going from such a file to actual instructions for a specific printer and printing material is called slicing for which several free programs exist. When a model is sliced there are many settings available for fine tuning the resulting print. A few of them are relevant to this project and will be discussed here. The slicing software used in this project are versions 15.04.6 Cura and 4.8.0 of Ultimaker Cura. [Ultimaker] The settings mentioned below are generic and should be available in most slicers.

The *layer height* sets the thickness of each layer of the print. A larger layer height will result in a faster print, but a smaller layer height will result in a more detailed print. It can be thought of as a way of setting the resolution in the Z direction.

The *nozzle size* is the diameter of the nozzle of the extruder. It determines the smallest printable feature in the X and Y directions, but the nozzle size is not a step size like the layer height is. The smallest step size in the X and Y direction depends on the motors and how those motors mechanically drive the axis. It is generally an order of magnitude smaller than the nozzle size and layer height and can be regarded as insignificant.

A *brim* is a feature that can be added to help the print stick to the bed. It is a wide border that is printed attached to the model on the first layer.

To help print overhangs mentioned previously, *support material* can be automatically generated. This material is some kind of structure that supports the overhang and should be relatively easy to remove when the print is done.

Chapter 4

Tactile Models

4.1 Modelling from Imaging Data

In this project only imaging data is turned into tactile models, the algorithm that creates them can however work for other types of three-dimensional data too. Because of this, the algorithm is discussed in this section in a more general approach. Unfortunately not all three-dimensional data can be directly turned into a printable model. A point cloud for example would be impossible to 3D print as the points would have to be suspended in the air. The method developed for this project can create a model of data that is complete over a two-dimensional grid and somewhat continuous in the third dimension.

The algorithm that creates the model takes a two-dimensional array $A_{m,n}$ of size n columns by m rows as input. Every element can be regarded as a point in three-dimensional space, where for element $a_{i,j}$ the x and y coordinate are proportional to i and j respectively and the z coordinate is proportional to the value of the element. A surface can then be created by looping over every element in the array except for the last row and column and creating two triangles for each element. As shown in figure 4.1 for element $a_{i,j}$ the first triangle has vertices $(i, j, a_{i,j})$, $(i + 1, j, a_{i+1,j})$ and $(i + 1, j + 1, a_{i+1,j+1})$ and the second triangle has vertices $(i, j, a_{i,j})$, $(i, j + 1, a_{i,j+1})$ and $(i + 1, j + 1, a_{i+1,j+1})$. All these triangles combine to create a surface or mesh of the data. In order to make this a complete object the surface has to be closed without exposed edges, also called a manifold mesh. To achieve this a flat surface is added slightly below the lowest vertex and sides are made to bridge from this surface to the vertices on the edges, creating a baseplate underneath the image surface. The vertices of all created triangles are added in a specific order (clockwise or counter-clockwise), as this determines what is considered the inward and outward facing side of the triangles. The resulting triangle mesh can be exported as an STL file.

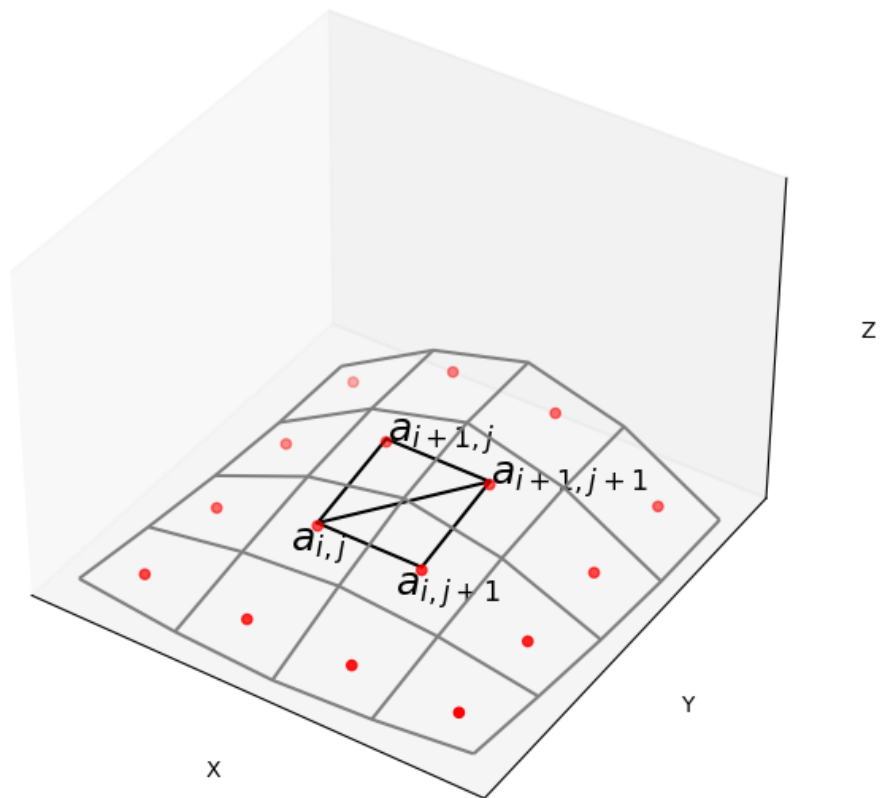


Figure 4.1: Drawing the mesh triangles for element $a_{i,j}$.

4.2 3D Printing Limitations and Solutions

To ensure successful and useful 3D printed tactile models, in this project best practices have been researched for the various steps in the process of going from initial image to the final tactile model. The found results will be described in this section.

4.2.1 Downscaling the image

As mentioned before, to be able to make a printable model the imaging data needs to be somewhat continuous. More specifically, the data needs to be continuous on the scale of the nozzle size of the 3D printer the model will be printed on. Features smaller than this size cannot be printed and may lead to unexpected or unrepresentative results when sliced. To prevent such features each image in this project is downscaled to a size where the size of one pixel is on the same order of magnitude as the nozzle size. Downscaling the image also prevents model files from becoming very large. The image is scaled by a factor of $\frac{1}{f}$ (only if $\frac{1}{f} < 1$) where

$$f = \left\lfloor \frac{\min(n_x, n_y)}{\lceil \max(x, y) / d_{nozzle} \rceil} \right\rfloor \quad (4.1)$$

In this equation, x and y are the size of the model in the X and Y dimension. n_x and n_y are the number of columns and rows in the image, respectively. Finally d_{nozzle} is the nozzle size which is set to a constant of 0.3 mm as this is a common size. This downscaling is not meant to be very precise, so an exact value for the nozzle size is not needed. The equation is designed so f will be as small as possible while still setting the size of a pixel to roughly the nozzle size. This is done to constrict the downscaling and prevent it from removing a lot of detail from the model.

The downscaling algorithm used in this project calculates the local mean of pixels in each block of size $f \times f$ in the image as the new value for one pixel. [van der Walt et al., 2014] The downscaling is applied as a last step before generating a mesh from the image, so all other image processing steps are applied to the original size image. Although this makes computing more heavy for some algorithms, it is needed. Because in some cases, such as removing foreground stars (see chapter 2.2), a downscaled image would severely hinder the quality of the output image.

4.2.2 Printer and model settings

Although tuning printer settings is a complicated task that varies hugely from printer to printer as well as between different materials, some general settings can be advised that should work in most cases. Of course, getting to know the best settings for a particular printer and material will yield

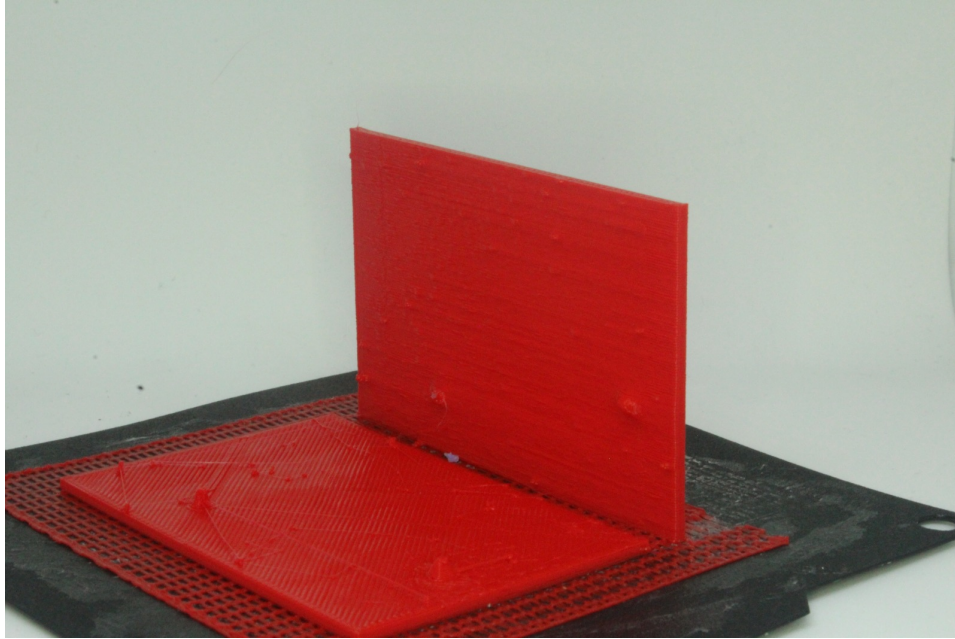


Figure 4.2: A print in landscape orientation (left) and one in portrait orientation (right).

better results, but with these basic settings anyone should be able to print a model regardless of printer or material.

Print orientation

Because of the nature of FFF 3D printing, how the model is oriented when it is printed has a big effect on things like the quality of the model and required printing time. For this project the distinction will be made between two main print orientations, which will be called *landscape* and *portrait*. Here, landscape orientation refers to the plane of the image being flat on the XY-plane of the printer and the brightness direction being along the Z-axis of the printer. The portrait orientation refers to the model being with one of its thin sides on the XY-plane of the printer and the plane of the image being along the Z-axis of the printer. The orientations can be seen in figure 4.2. Both orientations have their advantages and disadvantages.

Independent of other factors, like model size or set layer height, models in the landscape orientation the model will print faster ¹. This is because the height in the Z-axis of the printer contributes to how many layers the print has which in practice is one of the key parameters that determine the print time. Models in the landscape orientation will never have overhangs because of the way the models are created in this project will always include material

¹For the printers used in this project (see chapter 3), print times for landscape models were on the order of 1 hour.

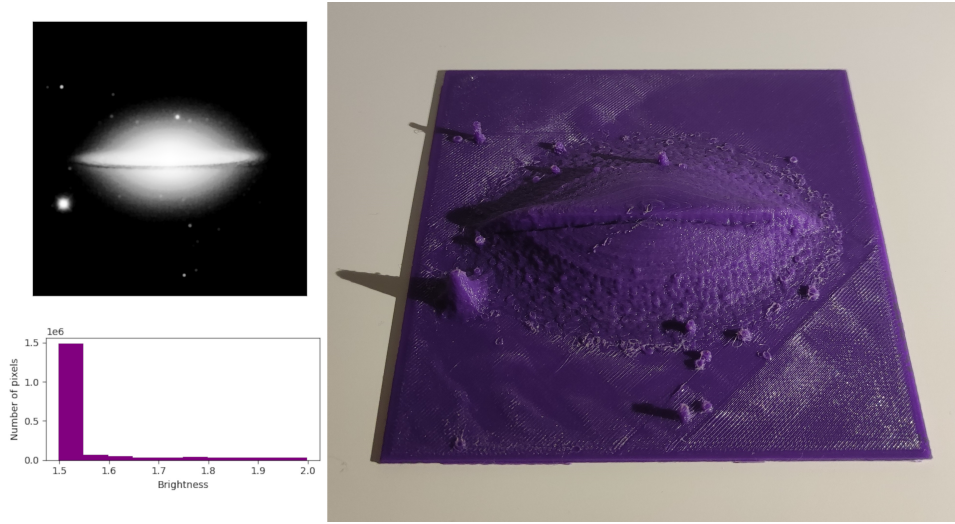


Figure 4.3: A tactile model of the Sombrero galaxy, generated from an image from the SDSS-3. [Aihara et al., 2011] The image was chopped at a floor value, the histogram was equalized, the image was log and gamma corrected and foreground stars were removed. The processed image and histogram are displayed to the left of the model. The model has a size of 100 mm by 100 mm by 10 mm high with a 1 mm thick baseplate added. It was printed in the landscape orientation.

from the baseplate up to the model’s top surface. Another advantage of this orientation is that it prints well also at large model heights, meaning models can be printed that show different brightness levels over a large range of distance. An example of such a model can be seen in figure 4.3.

The landscape orientation also has disadvantages, one being that the vertical resolution is limited to the layer height set on the printer. Although the layer height can be set, as discussed in chapter 3.2, it is generally about an order of magnitude larger than the smallest step size in the XY-plane. This means that models of a small height will have a small resolution of brightness levels. Another problem that can occur easily in landscape orientation is stringing, as for example stars can create a lot of different features on the XY-plane. Two examples of models with both of these issues can be seen in figure 4.4. One last possible issue with printing in landscape mode is that if the print is not cooled enough, the heat of the plastic and the extruder could propagate down and cause very small features to melt. This will depend on the type of printer, as most have a cooling fan to prevent this issue.

In the portrait orientation models can be printed with a higher resolution in the brightness direction. Because of this they are better suited for models of lower height. Portrait oriented models will never have stringing, as they

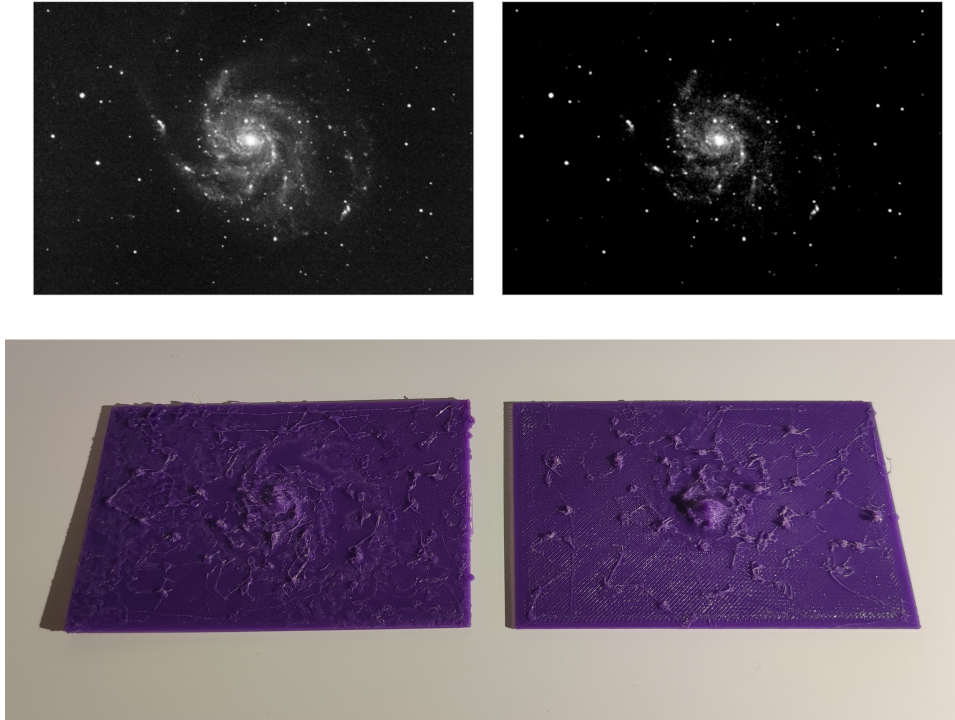


Figure 4.4: Two tactile models of M101. The image these models were generated from were chopped at a floor value, the histogram was equalized, the image was log corrected and only on the right model foreground stars were removed. The processed images are displayed above their corresponding models. The models have a width and height of 75 mm by 50 mm. The left model is 2 mm high and the right model 4 mm, both with a 1 mm thick baseplate added. They were printed in the landscape orientation.

always have a continuous contour with no separate features in the XY-plane. An example of a portrait orientation model can be seen in figure 4.5.

A disadvantage of portrait mode is that print times will take longer ², because of the much larger height of the print. Also in portrait orientation all bright features are overhangs. This limits the size of the model in the brightness direction, as small overhangs are usually printable. Support material could be used to support larger overhangs, but removing it could damage small features and doesn't leave a nice surface finish. It's therefore recommended that portrait models are printed with a brightness height that the printer is able to print without support material. On models with steep edges (caused by sudden changes in brightness) it is recommended that the model is rotated to stand on the edge that minimizes overhang.

Bed adhesion and stability

To ensure the model stays adhered to the bed a brim can be used, this is recommended for both printing orientations. In the case of landscape orientation a brim can prevent the model from warping as the print bottom layers of the print cool during printing. However, depending on the model size, material, printer and other print settings, this may not be necessary. Landscape models can have very thin baseplates as they will be very stable on the bed. But with a thin baseplate on a printer with a heated bed they should be left to cool before removing, since they might warp or bend while being removed otherwise.

Since portrait models have a small footprint on the bed to begin with, a brim is strongly recommended to make them more stable. Increasing the size of the baseplate also helps, as it directly increases the footprint and adds rigidity. Depending on the printer and how it drives the X and Y-axis, the stability of the model could be increased by aligning the long edge of the footprint to be parallel with either axis or on a 45 °angle to both.

4.2.3 Image Processing

Some of the image processing algorithms used in this project can be applied to increase the quality of the tactile model. This goal can sometimes work together with the goal creating a better quality image, but in some cases they are opposites. In this section it is assumed that image processing has already been done to make a good quality image. The processing can then be tweaked or more steps can be applied to improve the tactile model.

Landscape

For models in the landscape orientation it is very important to both remove noise and foreground stars, because both of these lead to stringing.

²For the printers used in this project (see chapter 3), print times for portrait models were on the order of 2 hours.



Figure 4.5: Tactile model of M51. The image was chopped at a floor and ceiling value, the histogram was equalized, the image was log corrected and denoised. The processed image is displayed above the model. The model was generated to have a size of 75 mm by 50 mm by 3 mm with a 2 mm thick baseplate added. It was printed in the portrait orientation.

Some stringing on a model is not a problem, but a lot can make it difficult to feel the actual surface of the print. Since denoising and removing foreground stars both darken the image and reduce detail, that must be compensated for. Setting a chop with a ceiling value and log correction can both help to compensate for the darkening of the image. Setting the model height to be larger helps with showing more detail. An example of a landscape model with such settings can be seen in figure 4.6.

Portrait

For portrait models the main challenge is to make the image bright enough to make sure everything that should be distinguishable is. Setting a chop with a ceiling value and log correction help to accomplish this. The image Z height (height in the brightness direction) can be experimented with to find a maximum height at which a particular printer will still print overhangs.

4.2.4 Draft model

As models can take quite some time to print, especially in portrait orientation, it can be useful to first make a draft model that is printed quickly. This can be used to get an idea of what the final tactile model will look like and whether the image processing yields the desired results. For visually impaired or blind people a draft model can be a way to inspect the model in between processing steps if they are not able to see the image on a computer screen. Another reason to make a draft model is to help better understand the final tactile model. As shown by Hasper et al. [2015], starting with a low resolution model and adding detail in subsequent models can help people get used to the way tactile models convey information.

For a quick draft model the biggest impact in printing time comes from the model size, model height and layer height. Minimizing those parameters should be a priority. To make a draft model with less detail a number of algorithms can help. Chopping the image with a floor and ceiling and equalizing the histogram with fewer bins will increase the contrast of the model. Denoising and removing foreground stars are a good way to remove small features and only leave bigger objects and smoother surfaces. In figure 4.7 a simplified draft model and a high detail model can be seen side by side.

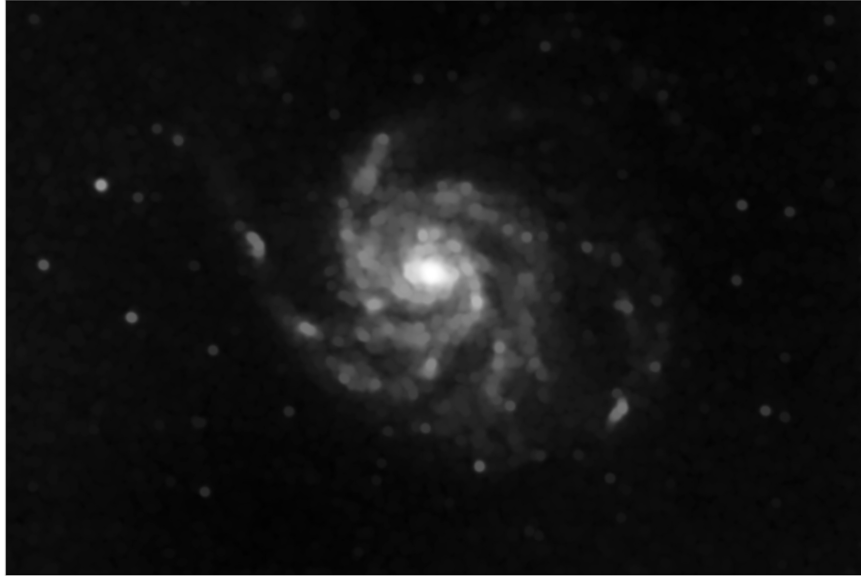


Figure 4.6: Tactile model of M101. The image was chopped at a floor and ceiling value, the histogram was equalized, the image was log corrected and foreground stars were removed. The processed image is displayed above the model. The model was generated to have a size of 100 mm by 67 mm by 10 mm with a 1 mm thick baseplate added. It was printed in the landscape orientation.

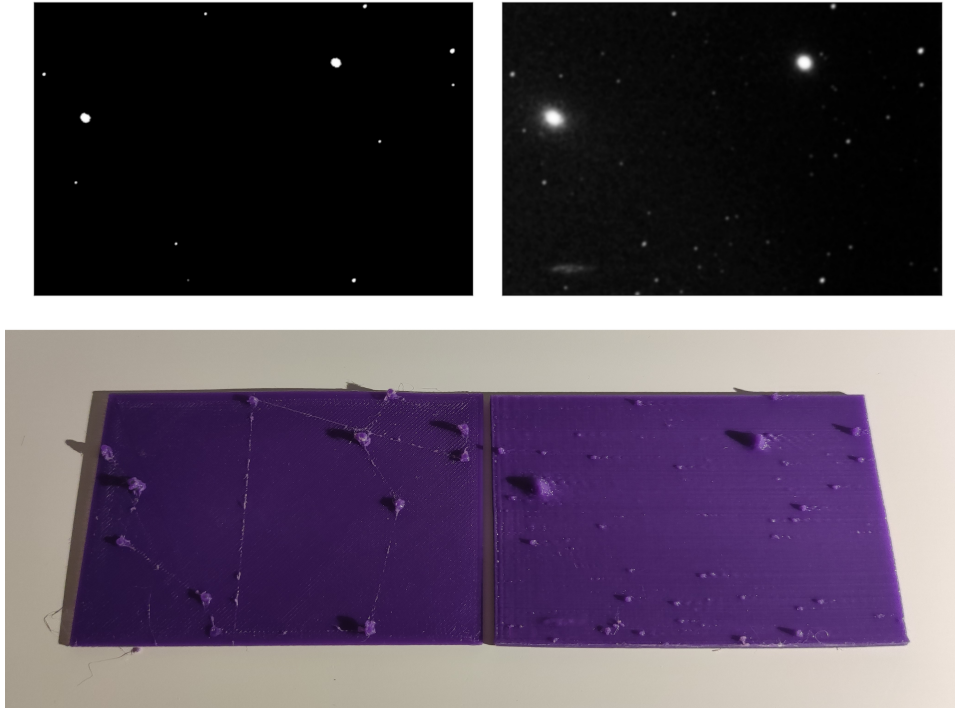


Figure 4.7: A draft tactile model and a high quality tactile model of the same image. The image is of M84 and M86. Both models were chopped at a floor and ceiling value, their histograms equalized and log corrected. For the draft model foreground stars were removed. For the high quality model the image was denoised. The processed images are displayed above their corresponding models. Both models have a size of 75 mm by 50 mm by 3 mm. To the draft model a 1 mm thick baseplate was added and it was printed in the landscape orientation. To the high quality model a 2 mm thick baseplate was added and it was printed in the portrait orientation.

Chapter 5

Interface

As a key goal of this project is to make the found procedures accessible, an effort has been made to provide an easy way to create tactile models such as discussed. Therefore, an interface program was made in which astronomical images can be processed and turned into tactile models ready to slice for 3D printing. Slicing has been left out as it is a process specific to a particular 3D printer and there are many free slicers available with much more options than could have been implemented in this project. The interface program is called Tactile Astronomical Imaging System, or TAIS, and is available for free ¹ online ² under the GNU General Public License version 3. [van Beers and Noel-Storr, 2021] [Free Software Foundation, 2007] TAIS is written in Python using the `wxPython` graphical user interface toolkit, which was chosen because it supports most operating systems and because it is compatible with screenreaders. [The wxPython Team] This means that the interface can also be used by visually impaired or blind people as all text and interface elements are described. In the rest of this chapter an overview of the interface will be given.

5.1 Main window

The TAIS interface consists of one window with three panels. The window also has a toolbar from which the program can be quit or a FITS image file can be opened. The three panels in the window are the image preview panel, the processing queue panel and the model settings panel. A screenshot of the TAIS main window can be seen in figure 5.1.

¹Both "Free as in freedom" and "Free as in beer".

²<https://github.com/PracticalAstronomyCrew/fits-3dmodeller>



Figure 5.1: A screenshot of the TAIS interface, with an image of M51 loaded and processed.

5.2 Panels

The image preview panel shows a the opened image as well as it's histogram. When no image is opened, the view is blank. Below the image and histogram is a button to reset the view to input data. This can be useful as the image preview will show the processed image if algorithms are applied.

The processing queue panel is empty when the program is started, apart from two buttons. One button will add a process, another will apply the processing to the image. When the "Add process" button is pressed a new panel will appear within the processing queue panel for the new process. This panel has buttons to move the process up and down in the queue as well as one to remove it, it also has a drop down menu to select the type of process. The process types are all the algorithms described in chapter 2.2, for each algorithm the panel will include interface elements to set the adjustable parameters. When the "Apply processing" button is pressed the algorithms in the processing queue are applied to the opened image from top to bottom and the processed image appears in the image preview panel. If the button is pressed again, the processing is applied to the original input image - not to the previously processed image.

The model settings panel has input boxes for setting the X and Y size of the model in millimetres. There is also a checkbox to set the model size to be proportional to the image. If this checkbox is set, changing either the X or Y size will automatically update the other such that the model will be proportional to the image. There is in input box for setting the Z heigth in millimetres, this is the height difference in the model between the darkest

and the brightest area. There is also an input box to set the height of the baseplate. The Z height and baseplate height added together is the total height of the model. Finally, there is a button to make and save an STL model. This button will open a dialogue window where a file location and filename can be set for the exported STL file.

Chapter 6

Conclusion & Discussion

In this thesis methods have been researched to turn astronomical imaging data into 3D printed tactile models suitable for use by both sighted and visually impaired or blind users. These methods consist of image processing for better image quality, image processing for better model quality, model settings en 3D print settings. The only preprocessing of the data assumed is that for observational effects. Best practices for the image processing steps for both image and model quality have been discussed in the form of algorithms to apply in specific cases as well as how to balance the two. Also, it has been specified how to adjust the image processing for different model and print settings. For the different desired properties of tactile models in this project, model and print settings have been explained. To arrive at these best practices around 20 tactile models have been 3D printed from imaging data and many more have been generated. As accessibility was a key focus of this thesis, an interface has been created to make it easier to apply the methods discussed. The interface covers the entire process from imaging data to STL model, only excluding the slicing for 3D printing as this differs per 3D printer. Keeping BVI users in mind, the framework the interface was built with was specifically chosen because it is compatible with screenreaders.

In this thesis the generated models were not evaluated with users, which would have been valuable to gather some quantitative data on the how well the tactile models served their purpose. Instead for this project the available time was focussed more on accessibility and creating the interface, resulting in a tool that can be used by specific users in specific use cases to create personalised tactile models. There are still a number of improvements possible for the interface. In this project only a few image processing algorithms were used, many more could be implemented. In terms of accessibility, although the interface can be read with screenreaders, it is difficult to guess the right parameters for image processing if the user can't see the image preview. Being able to enlarge the image would be a valuable improvement for visu-

ally impaired users. To help BVI users that cannot see the image preview, some audible way of conveying the information in the histogram could be experimented with. Also, further research could be done to see what image processing and model settings are effective for different use cases and users. There could then be an option to load these predetermined settings. As the interface was created in a short time frame, more work could be done on the layout and overall stability of the program. It could then be exported to executables to make installing it easier for users.

Bibliography

H. Aihara, C. Allende Prieto, D. An, S. F. Anderson, É. Aubourg, E. Balbinot, T. C. Beers, A. A. Berlind, S. J. Bickerton, D. Bizyaev, M. R. Blanton, J. J. Bochanski, A. S. Bolton, J. Bovy, W. N. Brandt, J. Brinkmann, P. J. Brown, J. R. Brownstein, N. G. Busca, H. Campbell, M. A. Carr, Y. Chen, C. Chiappini, J. Comparat, N. Connolly, M. Cortes, R. A. C. Croft, A. J. Cuesta, L. N. da Costa, J. R. A. Davenport, K. Dawson, S. Dhital, A. Ealet, G. L. Ebelke, E. M. Edmondson, D. J. Eisenstein, S. Escoffier, M. Esposito, M. L. Evans, X. Fan, B. Femenía Castellá, A. Font-Ribera, P. M. Frinchaboy, J. Ge, B. A. Gillespie, G. Gilmore, J. I. González Hernández, J. R. Gott, A. Gould, E. K. Grebel, J. E. Gunn, J.-C. Hamilton, P. Harding, D. W. Harris, S. L. Hawley, F. R. Hearty, S. Ho, D. W. Hogg, J. A. Holtzman, K. Honscheid, N. Inada, I. I. Ivans, L. Jiang, J. A. Johnson, C. Jordan, W. P. Jordan, E. A. Kazin, D. Kirkby, M. A. Klaene, G. R. Knapp, J.-P. Kneib, C. S. Kochanek, L. Koesterke, J. A. Kollmeier, R. G. Kron, H. Lampeitl, D. Lang, J.-M. Le Goff, Y. S. Lee, Y.-T. Lin, D. C. Long, C. P. Loomis, S. Lucatello, B. Lundgren, R. H. Lupton, Z. Ma, N. MacDonald, S. Mahadevan, M. A. G. Maia, M. Makler, E. Malanushenko, V. Malanushenko, R. Mandelbaum, C. Maraston, D. Margala, K. L. Masters, C. K. McBride, P. M. McGehee, I. D. McGreer, B. Ménard, J. Miralda-Escudé, H. L. Morrison, F. Mullally, D. Muna, J. A. Munn, H. Murayama, A. D. Myers, T. Naugle, A. F. Neto, D. C. Nguyen, R. C. Nichol, R. W. O'Connell, R. L. C. Ogando, M. D. Olmstead, D. J. Oravetz, N. Padmanabhan, N. Palanque-Delabrouille, K. Pan, P. Pandey, I. Pâris, W. J. Percival, P. Petitjean, R. Pfaffenberger, J. Pforr, S. Phleps, C. Pichon, M. M. Pieri, F. Prada, A. M. Price-Whelan, M. J. Raddick, B. H. F. Ramos, C. Reylé, J. Rich, G. T. Richards, H.-W. Rix, A. C. Robin, H. J. Rocha-Pinto, C. M. Rockosi, N. A. Roe, E. Rollinde, A. J. Ross, N. P. Ross, B. M. Rossetto, A. G. Sánchez, C. Sayres, D. J. Schlegel, K. J. Schlesinger, S. J. Schmidt, D. P. Schneider, E. Sheldon, Y. Shu, J. Simmerer, A. E. Simmons, T. Sivarani, S. A. Snedden, J. S. Sobeck, M. Steinmetz, M. A. Strauss, A. S. Szalay, M. Tanaka, A. R. Thakar, D. Thomas, J. L. Tinker, B. M. Tofflemire, R. Tojeiro, C. A. Tremonti, J. Vandenberg, M. Vargas Magaña, L. Verde, N. P. Vogt, D. A. Wake,

- J. Wang, B. A. Weaver, D. H. Weinberg, M. White, S. D. M. White, B. Yanny, N. Yasuda, C. Yèche, and I. Zehavi. The Eighth Data Release of the Sloan Digital Sky Survey: First Data from SDSS-III. *ApJS*, 193: 29, Apr. 2011. doi: 10.1088/0067-0049/193/2/29.
- J. Blackorby, M. Chorost, N. Garza, and A.-M. Guzman. *The academic performance of secondary school students with disabilities*. 2003.
- N. J. Bonne, J. A. Gupta, C. M. Krawczyk, and K. L. Masters. Tactile Universe makes outreach feel good. *Astronomy & Geophysics*, 59(1):1.30–1.33, 02 2018. ISSN 1366-8781. doi: 10.1093/astrogeo/aty028. URL <https://doi.org/10.1093/astrogeo/aty028>.
- B. Cavenaugh, M. Giesen, and B. Steinman. Contextual effects of race or ethnicity on acceptance for vocational rehabilitation of consumers who are legally blind. *Journal of Visual Impairment and Blindness*, 100:425–436, 07 2006. doi: 10.1177/0145482X0610000706.
- A. Chambolle. An algorithm for total variation minimization and applications. *Journal of Mathematical Imaging and Vision*, 20(1):89–97, Jan 2004. ISSN 1573-7683. doi: 10.1023/B:JMIV.0000011325.36760.1e. URL <https://doi.org/10.1023/B:JMIV.0000011325.36760.1e>.
- D. J. Eisenstein, D. H. Weinberg, E. Agol, H. Aihara, C. Allende Prieto, S. F. Anderson, J. A. Arns, E. Aubourg, S. Bailey, E. Balbinot, and et al. SDSS-III: Massive Spectroscopic Surveys of the Distant Universe, the Milky Way, and Extra-Solar Planetary Systems. *AJ*, 142:72, Sept. 2011. doi: 10.1088/0004-6256/142/3/72.
- Free Software Foundation. Gnu general public license, version 3. <http://www.gnu.org/licenses/gpl.html>, June 2007. Last retrieved 2021-07-01.
- E. Hasper, R. A. Windhorst, T. Hedgpeth, L. V. Tuyl, A. Gonzales, B. Martinez, H. Yu, Z. Farkas, and D. P. Baluch. Methods for creating and evaluating 3d tactile images to teach stem courses to the visually impaired. *Journal of College Science Teaching*, 44(6):92–99, 2015. ISSN 0047231X, 19434898. URL <http://www.jstor.org/stable/43632001>.
- R. Jones, P. Haufe, E. Sells, P. Iravani, V. Olliver, C. Palmer, and A. Bowyer. Reprap – the replicating rapid prototyper. *Robotica*, 29(1):177–191, 2011. doi: 10.1017/S026357471000069X.
- LABIST. Labist x1. <https://labists.com/products/mini-3d-printer-labists-x1>.
- H. Pashler, M. McDaniel, D. Rohrer, and R. Bjork. Learning styles: Concepts and evidence. *Psychological Science in the Public Interest*, 9(3):105–119, 2008. doi: 10.1111/j.1539-6053.2009.01038.x.

- URL <https://doi.org/10.1111/j.1539-6053.2009.01038.x>. PMID: 26162104.
- J. Prusa. Prusa mendel iteration 2. https://reprap.org/wiki/Prusa_Mendel, November 2011.
- A. C. Rule. Tactile earth and space science materials for students with visual impairments: Contours, craters, asteroids, and features of mars. *Journal of Geoscience Education*, 59(4):205–218, 2011b. doi: 10.5408/1.3651404. URL <https://doi.org/10.5408/1.3651404>.
- A. C. Rule, G. P. Stefanich, R. M. Boody, and B. Peiffer. Impact of adaptive materials on teachers and their students with visual impairments in secondary science and mathematics classes. *International Journal of Science Education*, 33(6):865–887, 2011a. doi: 10.1080/09500693.2010.506619. URL <https://doi.org/10.1080/09500693.2010.506619>.
- M. Sahin and N. Yorek. Teaching science to visually impaired students: A small-scale qualitative study. *Online Submission*, 6, 01 2009.
- J. E. Solem. Histogram equalization with python and numpy, 2009. URL <http://www.janeriksolem.net/histogram-equalization-with-python-and.html>.
- G. V. Tcheslavski. Morphological image processing: Gray-scale morphology. 2010.
- The wxPython Team. wxpython. URL <https://www.wxpython.org/>.
- Ultimaker. Ultimaker/cura. URL <https://github.com/Ultimaker/Cura/tags>.
- T. van Beers and J. Noel-Storr. PracticalAstronomyCrew/fits-3dmodeller: First release, July 2021. URL <https://doi.org/10.5281/zenodo.5057512>.
- S. van der Walt, J. L. Schönberger, J. Nunez-Iglesias, F. Boulogne, J. D. Warner, N. Yager, E. Gouillart, T. Yu, and the scikit-image contributors. scikit-image: image processing in Python. *PeerJ*, 2: e453, 6 2014. ISSN 2167-8359. doi: 10.7717/peerj.453. URL <https://doi.org/10.7717/peerj.453>.
- M. Yuen, P. Westwood, and G. Wong. Meeting the needs of students with specific learning difficulties in the mainstream education system: Data from primary school teachers in hong kong. *International Journal of Special Education*, 20:67–76, 01 2004.